2010 American Control Conference
Marriott Waterfront, Baltimore, MD, USA
June 30-July 02, 2010

A Control Architecture Solution to Superheat Nonlinearity

Matthew S. Elliott, Bhaskar Shenoy, and Bryan P. Rasmussen

***Abstract*— Evaporator superheat control is an important aspect of the operation of refrigeration and air conditioning systems; since the majority of cooling in these systems occurs through evaporation of two-phase refrigerant, the energy efficiency is improved by reducing the amount of superheat present. However, allowing refrigerant to leave the evaporator without completely vaporizing risks catastrophic damage to the compressor, so superior control is required at low superheat levels. One of the most significant challenges present in this control problem is the presence of significant nonlinearities in the response from the control input, e.g. expansion valve position, to evaporator superheat. This paper reveals how a particular control architecture inherently compensates for both the static and dynamic nonlinearities that dominate the valve-to-superheat transient response. Furthermore, the control implementation only requires temperature measurements, which are frequently available in ordinary HVAC systems. Modeling and experimental results confirm the reduction of nonlinearities using the proposed approach, and the authors discuss the effect of actuator limitations on the nonlinearity compensation.**

I. Introduction

Vapor compression cycle (VCC) systems are the primary tool for air conditioning and refrigeration in the United States, and heating, ventilation, air conditioning, and refrigeration (HVAC&R) systems account for 40% of United States commercial energy consumption [1]. One of the primary system parameters that affects system efficiency is evaporator superheat; thus, better superheat control can have a significant impact on energy consumption by these systems. Superheat control is a difficult problem, largely due to the nonlinearities present in all VCC systems. This difficulty is compounded by the lack of complete measurement of system states in typical systems, and by the lack of a priori knowledge of the system components parameters, e.g. valve flow characteristics, which render traditional feedback linearization schemes cumbersome to implement. The primary contribution of this paper is a control architecture that addresses these problems by compensating for system nonlinearities using a cascaded feedback loop, while only requiring measurements typically available for use, namely, refrigerant pressures and temperatures.

The ideal VCC consists of four processes: 1) isentropic compression, 2) isobaric heat rejection and condensation, 3) isenthalpic expansion, and 4) isobaric heat absorption and evaporation. Fig. 1 shows the cycle components for an ideal VCC; Fig. 2 is a typical pressure-enthalpy (P-h) curve for a refrigeration cycle.

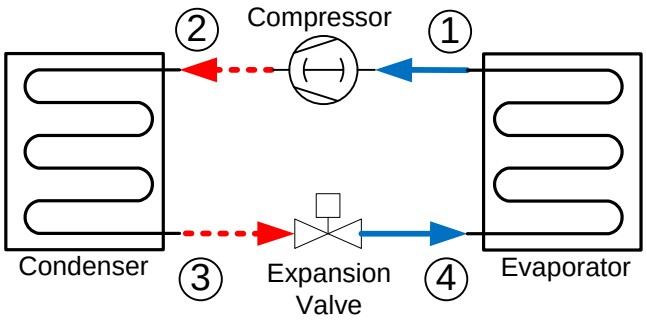

Fig. 1. Vapor compression cycle (VCC) components.

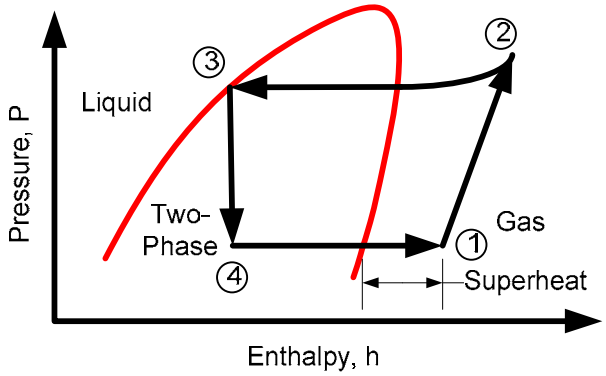

Fig. 2. Pressure-enthalpy (P-h) diagram.

Evaporator superheat is defined to be the difference between the refrigerant temperature at the evaporator outlet and the evaporator saturation temperature. Superheat control is a critical control problem for VCC-based systems, both in terms of optimizing system efficiency and preventing component failure. As the fluid passes through the evaporator, it absorbs heat and transitions from a liquid-gas mixture to a saturated vapor, and then further to a superheated vapor. If the refrigerant is allowed to leave the evaporator without completely vaporizing (i.e., no superheat), it will enter the compressor as a two-phase mixture, with the potential of causing catastrophic failure of the compressor. However, since the majority of the heat transfer occurs during the vaporization process, excessively high superheat results in reduced cooling capacity of the system. Therefore, the portion of two-phase flow in the

Manuscript received September 22, 2009. This work was supported in part by NSF CAREER Grant CMMI-0644363.

Matthew S. Elliott is a graduate researcher with the Texas A&M University Department of Mechanical Engineering, College Station, TX.

Bhaskar Shenoy is a graduate researcher with the Texas A&M University Department of Mechanical Engineering, College Station, TX.

Bryan P. Rasmussen is an Assistant Professor of Mechanical Engineering at Texas A&M University, College Station, TX. (phone: 979-862-2776, fax: 979-845-3081, email: brasmussen@tamu.edu)

evaporator should be maximized in order to obtain maximum cooling capacity of the system. In general, an acceptable compromise between efficiency and safety is for the refrigerant at the evaporator exit to be a few degrees above its saturation temperature. Regulating this temperature difference is called superheat control, a perennial control problem for HVAC&R applications.

II. Superheat Control

Superheat control is a fluid metering problem. The metering of refrigerant in air conditioning, refrigeration, or heat pump systems is generally achieved by a number of different valve types, which vary in expense and design sophistication. The primary refrigerant metering device is known as the expansion valve, so called because the fluid expands from the liquid phase to a two-phase fluid mixture as the refrigerant travels through the valve, transitioning to a lower pressure. The simplest of expansion valve devices is a capillary tube or orifice tube where the refrigerant flows through a reduction in diameter. Other mechanical control devices include a thermostatic expansion valve (TEV) or a pressure regulating device also known as an automatic expansion valve (AEV). Expansion valves that are actively controlled by a computer-based algorithm include the electronic expansion valve (EEV), which is opened and closed by a stepper motor.

The electronic expansion valve (EEV) was a major step forward in superheat control, since it allows the implementation of automatic control paradigms such as Proportional-Integral-Derivative (PID). The EEV consists of a needle valve with a stepper motor to adjust the valve position. Fig. 3 is a schematic of the EEV.

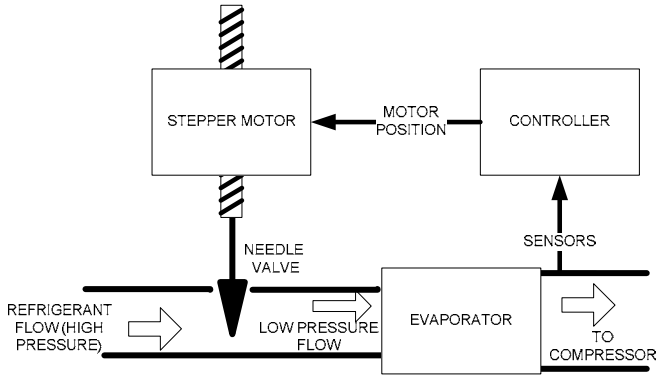

Fig. 3: EEV construction

Since the EEV uses electronic controllers that can be tuned, problems with mechanical devices such as valve hunting can be overcome. In [7] the authors use a simplified identified model for the evaporator, and then compare PID and optimal control algorithms. Similarly in [3] the authors design a PID controller based on a simplified identified model for the evaporator, and compare PID control to the TEV.

Design of EEV control algorithms is complicated by the inherent nonlinear dynamics, leading many researchers to suggest that scheduling of controller gains is necessary to effective operation ([3], [7]). Additionally, the work of H. Rasmussen et al implemented a cascaded control architecture, wherein an inner loop regulated the refrigerant mass flow to a setpoint generated by a linear PID controller seeking to regulate superheat; this approach significantly linearized the response of the evaporator to the controller, although it requires refrigerant flow measurements, which are not typically available in refrigeration systems [8]. A method for characterizing and cancelling static nonlinearities (such as that found in EEVs) is presented in [9]. A feedback linearization approach to HVAC control that required a system model was also presented in [5]. The interested reader can find a survey of linearization through feedback in [4].

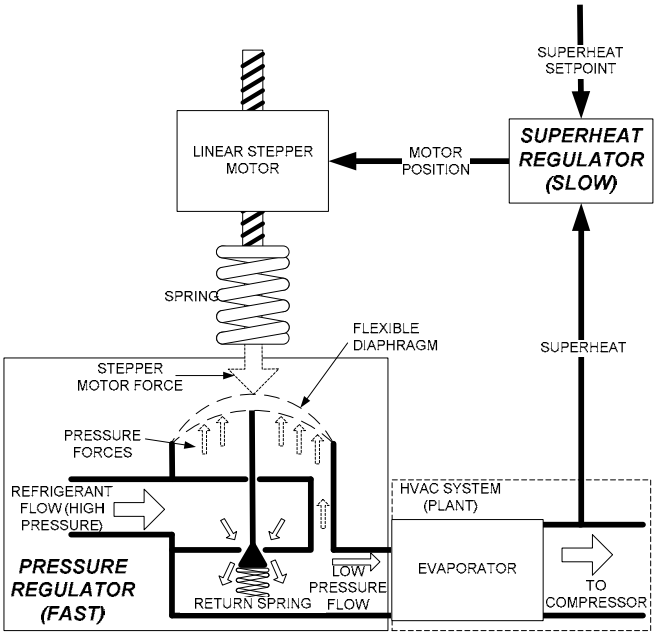

Fig. 4: HEV construction

In [2] the authors proposed a Hybrid Expansion Valve (HEV) that regulates fluid flow based on both pressure and superheat measurements, resulting in superior transient regulation. The novel combination of mechanical and electronic regulation mechanisms offers several advantages including greater anticipated device longevity due to significantly decreased electronic actuation. Fig. 4 shows the HEV's construction. In order to compare the disturbance rejection of the two actuators, the VCC system was subjected to a series of disturbances imposed by compressor speed changes. The compressor speed profile for the two tests is shown in Fig. 5. Each actuator was controlled with a well-tuned PID loop (see Table I for the controller gains). The superheat and actuator movements are shown in Fig. 6.

TABLE I: CONTROLLER GAINS

Control Loop	K_P	K_I	K_D
EEV-PID	2.5	0.25	0.2
HEV-PID	1.5	0.2	0.1

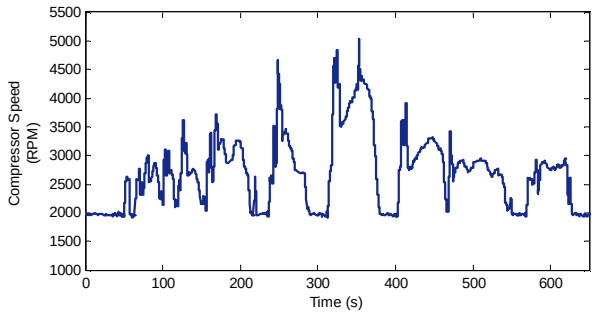

Fig. 5: Compressor speed profile.

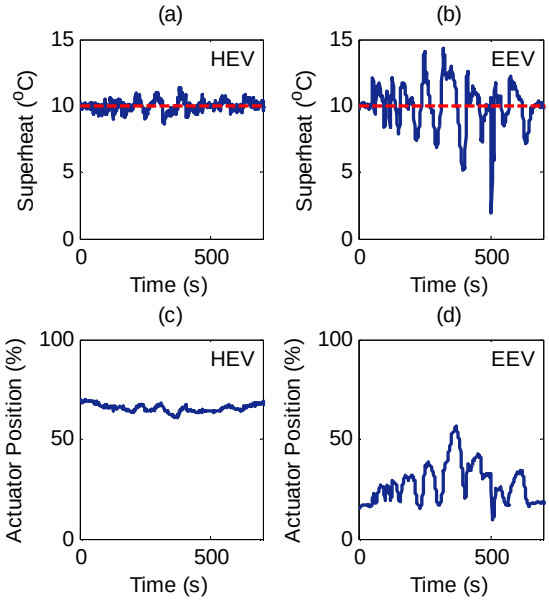

Fig. 6: Disturbance rejection by the two actuators for the compressor speed profile shown in Fig. 5. The graphs show superheat for the (a) HEV test, (b) EEV test, and the control input for (c) the HEV and (d) the EEV.

The HEV clearly provides superior disturbance rejection with much less actuator motion. Experimentation also revealed that in addition to superior disturbance rejection, the HEV also partially compensates for system nonlinearities; this is a significant improvement, since the ability to compensate for system nonlinearities could greatly simplify the control design task, and lead to better performance and efficiency over a wider range of operating conditions. The nonlinearity compensation is due to the cascaded control structure of the HEV; similar results can also be replicated with a traditional EEV, which is in general not a linear actuator. The rest of the paper is organized as follows. First, a discussion will use both experimental results and modeling to show that the EEV's inherent static nonlinearities are the most significant driving force in the overall nonlinear behavior in the evaporator. Next, a cascaded control architecture is proposed that compensates for the EEV's nonlinearities while only using signals frequently available for measurement in standard VCC systems. Further modeling efforts verify that the control architecture significantly reduces the static and dynamic nonlinearities of the system. Finally, experimental results display the efficacy of the approach.

III. EEV Nonlinearities

Inspection of refrigerant mass flow as a function of valve position for a typical EEV reveals a nonlinear relationship, as shown in Fig. 7(a). Fig. 7(b) shows superheat responses to EEV step changes for high refrigerant flow and low refrigerant flow conditions. Clearly, the response is much different for the EEV at high and low flow conditions. This is caused by the same step change causing different changes in flow depending on the valve position. This nonlinearity in the EEV means that adequate superheat control is much more difficult to achieve for this device, and illustrates why a gain scheduling approach based upon the different flow conditions is frequently used. Alternatively, the controller can be "de-tuned," sacrificing performance for stability over all operating regions due to smaller control gains; however, this risks losing superheat during system transients.

Using a static inversion mapping between command signal and valve position [6], refrigerant flow was linearized, similar to the work presented in [9]. This resulted in a much smaller difference in step response for the different conditions, although differences in dynamic response are still evident. See Fig. 8.

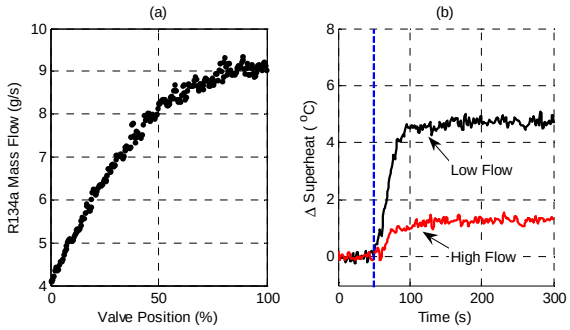

Fig. 7. Nonlinear EEV: (a) Mass flow vs. Valve position static map, and (b) Step responses for low and high flows

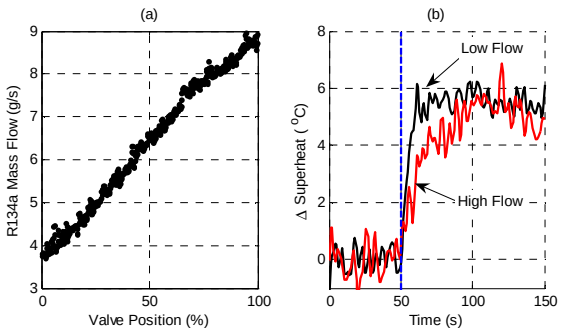

Fig. 8. Linearized EEV: (a) Mass flow vs. Valve position static map, and (b) Step responses for low and high flows

The above experimental results primarily give insight into the steady state responses of superheat to valve position. To develop a deeper understanding of the dynamic characteristics, a mathematical model was used to explore the responses at different flow rates for both the nonlinear and linear EEVs.

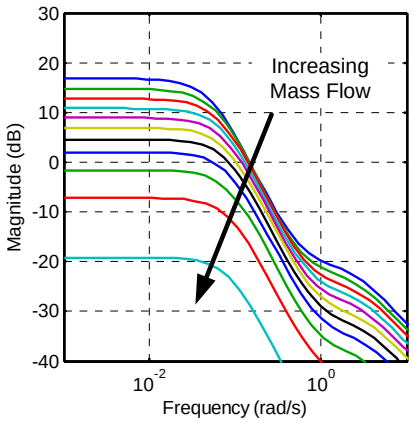

Fig. 9. Bode plots of the nonlinear EEV to superheat transfer function for different flow rates. As the flow rate increases, the steady state gain decreases.

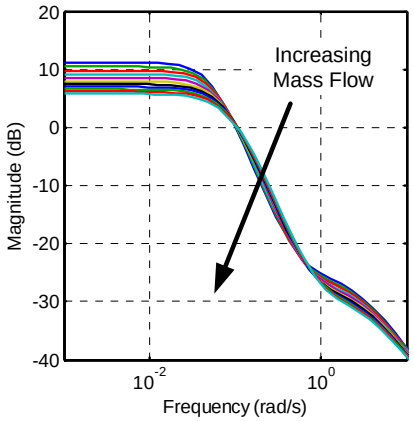

Fig. 10. Bode plots of the linear EEV to superheat transfer function for different flow rates Note the much smaller spread in gains and dynamics than the nonlinear valve.

The plant model used to compare the linear and nonlinear EEV responses consists of individual models for the EEV, compressor, evaporator, and condenser. The valve model assumes an isenthalpic expansion process, with the refrigerant mass flow rate being calculated from the standard orifice equation. The valve coefficient of discharge is taken from a semi-empirical map, which gives the coefficient as a function of the valve's pressure drop and the valve opening. The compressor model assumes an adiabatic compression process with the volumetric and adiabatic efficiency calculated using semi-empirical maps as a function of the pressure ratio and the compressor speed.

The evaporator and condenser heat exchanger models are based upon the moving boundary modeling approach ([10], [11]), which uses a time varying boundary separating the different refrigerant phases in the heat exchanger. The heat exchangers' heat transfer coefficients are calculated using the Wattelet-Chato correlation for two phase evaporating flows [14], the Dobson-Chato correlation for condensing two-phase flows [15], and the Gnielinski correlation for single phase flows [12].

The nonlinear models for the valve, compressor and heat exchanger are linearized about a given operating condition using a first-order Taylor series expansion. The linearized equations are combined to form the required plant model for the given operating condition [13].

Figs. 9 and 10 show a series of Bode plots for high and low flow conditions for two different EEVs—one with a static nonlinearity (Fig. 9), and one with a linear relationship between valve position and mass flow (Fig. 10). These two plots correlate with Figs. 7 and 8, respectively. As with the experimental results, the difference in static gain from valve position to superheat is significantly reduced with a linear mapping. Furthermore, the bandwidths are much more similar for the linearized valve than for the nonlinear valve.

These results suggest that the flow characteristics of the EEV are the dominant cause of the nonlinearity of response at different conditions. Thus, if the refrigerant flow is a linear function of valve command, the resulting superheat response will be substantially linearized. This may render the use of gain scheduling unnecessary, since robust control techniques can then be employed without unacceptable decreases in control performance. However, since EEVs will not in general be linear in flow characteristics, and since mass flow measurements may not be available for development of static inversion maps, a method for linearizing the flow (and hence the superheat response) is needed that only requires more basic measurements such as pressure and temperatures. The cascaded control approach proposed herein meets these requirements.

IV. Cascaded Control

The cascaded approach to superheat control consists of two nested control loops, as shown in Fig. 11. The inner, "fast" loop uses a proportional controller with gain K_F that seeks to regulate the evaporator pressure to a setpoint (P_{SET}) generated by an outer, "slow" controller C(s). This pressure setpoint is chosen by the controller C(s) to regulate evaporator superheat to a user-defined setpoint. The relationship between valve position v and mass flow m is treated as a nonlinear gain function $K_M(v)$, and is a characteristic of the actuator used. The transfer functions G(s) and H(s) are the dynamic relationships from mass flow to superheat and pressure, respectively. Note that the only measurements necessary for implementation are refrigerant temperature at the outlet of the evaporator and evaporator pressure; since the refrigerant at the evaporator inlet is two-phase, its temperature can be found from pressure measurements using a lookup table, or the inlet temperature can be measured directly.

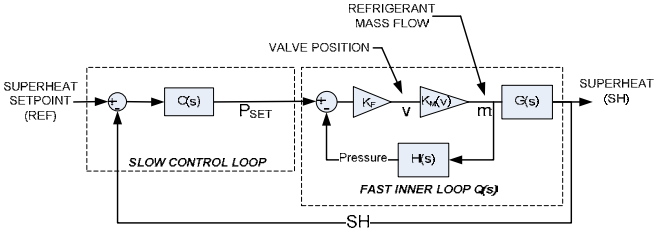

Fig. 11. Cascaded control loop architecture that emulates the HEV actuator.

The fast inner loop block diagram can be reduced to a transfer function Q(s):

$$Q(s) = \frac{SH}{P_{set}} = \frac{K_F K_M(v) G(s)}{1 + K_F K_M(v) H(s)} \quad (1)$$

Assuming stability allows invocation of the Final Value Theorem, which gives a value for the steady state gain of Q:

$$Q(0) = \frac{SH_{final}}{P_{set}} = \frac{K_F K_M(v) G(0)}{1 + K_F K_M(v) H(0)} = \frac{K(v) G(0)}{1 + K(v) H(0)} \quad (2)$$

Thus, if the steady state gains of G and H vary in the same direction as mass flow changes, e.g., they both decrease with increasing mass flows, then the variation of Q(0) as mass flow changes will be minimized as K(v) becomes larger. Experimental evaluation of the same EEV used earlier gave the following result, shown in Fig. 12. Clearly, the steady state responses of both G(s) and H(s) decrease with increasing mass flow. This implies that if the feedback gain in the fast loop is large enough, the cascaded architecture will give a reduction in the nonlinearity of response from the P_{SET} pressure setpoint to the evaporator superheat. The next section will present modeling results that this indeed is the case.

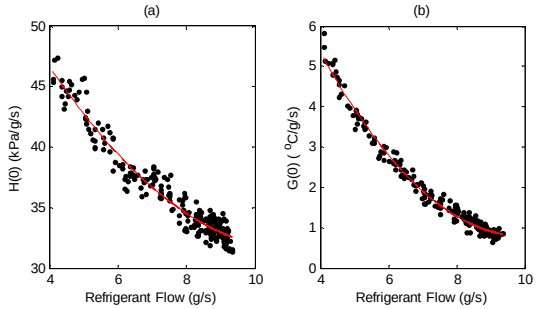

Fig. 12. Steady state gains varying with refrigerant mass flow for (a) Mass flow to evaporator pressure, and (b) Mass flow to evaporator superheat.

V. Cascaded Control Implementation

A. Modeling

The same modeling approach discussed in Section III was implemented with the cascaded control loop; this models the fast inner loop designated as Q(s) in Fig. 11. This transfer function treats the pressure setpoint P_{SET} as the input and superheat as the output. Fig. 13 is a set of Bode plots for this transfer function for different flow conditions, with a K_F value of 1.0. Fig. 14 is a similar plot, with a K_F of 10. Note that as K_F grows larger, the nonlinearity compensation becomes more pronounced. This agrees with the analytical prediction made in Section IV. For each case, the change in steady state values is significantly less than that of the nonlinear EEV as refrigerant flows vary.

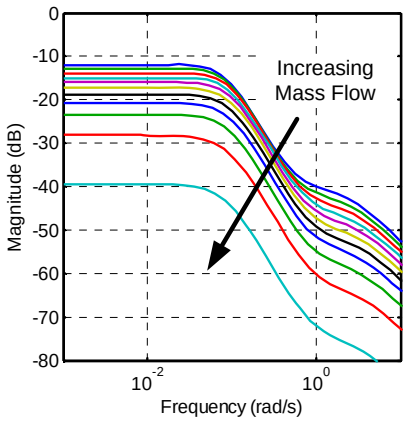

Fig. 13. Bode plots for Q(s), with K_F =1.

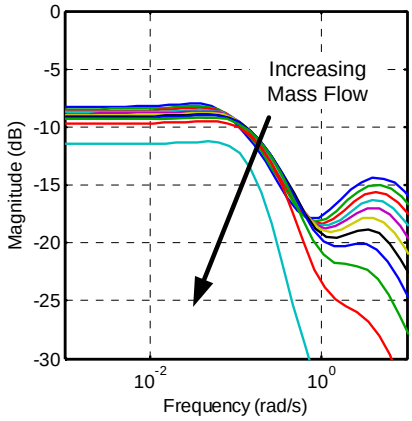

Fig. 14. Bode plots for Q(s), with K_F =10.

B. Experimental Data with Cascaded Control

In the implementation of the EEV as the cascaded loop actuator, a proportional gain K_F of 0.22 was used. A larger gain was not useable, since the delays and slew rate limit of the EEV rendered the closed loop plant unstable with a higher gain. The values of K for both HEV and cascaded EEV are plotted in Fig. 15, and are shown varying as the pressure setpoint changes, since the needle valve position v is not available for measurement in the HEV. The higher gain shown by the HEV means that the HEV will have better response and more nonlinearity compensation than the EEV, but the high gain results in large, fast valve movements.

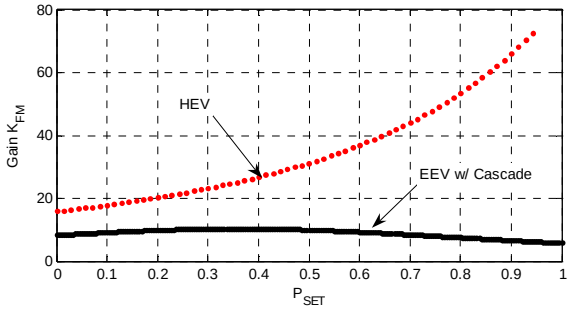

Fig. 15. Total loop gain for HEV and cascaded EEV. P_{SET} is scaled for easy comparison. The larger value for the HEV gives better compensation.

Since the proportional gain used with the EEV cannot be high enough to give an internal loop gain as high as that of the HEV, the EEV in cascaded configuration will not give the same degree of nonlinearity compensation as the HEV; this is illustrated in Fig. 16. The HEV (Fig. 16a) has a steady state difference of approximately 0.5° C between high and low flows; the EEV with cascaded control (Fig. 16b) has a difference of about 2.5° C. This is a significant improvement over the original case shown in Fig. 7, and shows that the cascaded control loop does indeed partially compensate for the nonlinearities of the system; additionally, the system exhibits much faster dynamic changes to the step response.

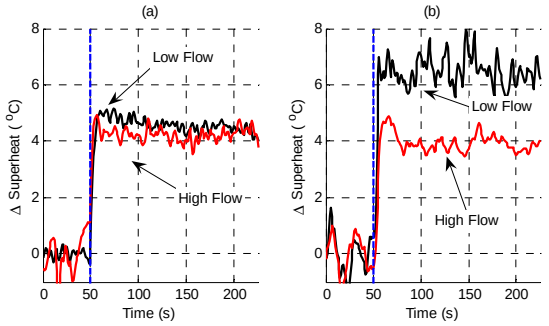

Fig. 16. Step responses for (a) HEV and (b) cascaded EEV. The higher degree of nonlinearity compensation of the HEV agrees with the prediction in Fig. 15.

These data show that the HEV's significantly higher gains contribute to a much higher degree of nonlinearity compensation than that of the cascaded EEV. However, attempting to recreate the HEV's performance by using its gains on the EEV-based cascaded loop resulted in an unstable system. This is due to the inherent delay and relatively slow response of the EEV. An actuator that responds slowly is said to have a low bandwidth; this places a physical limitation on the control schemes that can be implemented with the actuator. In this case, the EEV's bandwidth limits the gains that can be used in the internal proportional controller. Future research efforts will implement a micro-electrical-mechanical (MEMS) based expansion valve with the cascaded control structure. This actuator, which features a much higher bandwidth than the standard EEV, promises to combine the ease of implementation of the standard EEV with the high gains—thus greater nonlinearity compensation and faster response—of the HEV.

VI. Conclusion

Superheat control is an important problem in refrigeration and air conditioning systems; since good superheat regulation allows for more efficient operation of these systems, an improvement in this control can have a significant impact on worldwide energy usage. The nonlinearities present in these systems make control difficult, however. Experimental results showed that linearizing the flow rate as a function of valve position will linearize the superheat response; however, since EEVs are generally not linear and mass flow measurements may not always be available, this may not be a viable solution for most applications. This paper proposed a cascaded control algorithm that eliminates most of the nonlinearity of the response between algorithm-generated control input and the superheat output, while only requiring pressure and temperature measurements. This reduces the need for gain scheduling or other advanced control algorithms, and takes advantage of system measurements widely found in HVAC&R applications. The cascaded control approach was implemented using both an EEV and a "hybrid" expansion valve wherein the pressure regulation is handled mechanically. The mechanical pressure regulator functions much more quickly, i.e., it has a very large proportional gain, due to the stiff spring and diaphragm, and thus reduces nonlinearities. Using the EEV enables reduction of nonlinearities, but the same level of performance cannot be obtained due to inherent limitations—low bandwidth—of the actuator. This suggests the use of a faster actuator will yield better results, and enable successful implementation of a digital-only control mechanism.

References

[1] Anonymous, 2006. Annual Energy Review 2005. DOE/EIA-0384(2005). http://www.eia.doe.gov/emeu/aer/consump.html.

[2] Elliott, M., Walton, Z., Bolding, B., and Rasmussen, B., "Superheat Control: A Hybrid Approach," *HVAC&R Res.*, vol. 15., no. 6, pp. 1021-1043, 2009.

[3] Finn, D.P. and Doyle, C.J., "Control and Optimization Issues Associated with Algorithm-Controlled Refrigerant Throttling Devices," *ASHRAE Trans.*, vol. 106, pp. 524-533, 2000.

[4] Guardabassi, G.O. and Savaresi, S.M., "Approximate linearization via feedback—an overview," *Automatica*, vol. 37, pp. 1-15, 2001.

[5] He, X.D. and Asada, H.H., "A New Feedback Linearization Approach to Advanced Control of Multi-Unit HVAC Systems," *Proc. of 2003 Amer. Cont. Conf.*, pp. 2311-2316, Denver, CO.

[6] Juricic, D., Strmcnik, S., Petrovcic, J., "Compensator for Static Nonlinearities—Design and Application," *Electronics Letters*, vol. 22., No. 10, pp. 532-534, 1986.

[7] Outtagarts, A., Haberschill, P., and Lallemand, M., "Transient Response of an Evaporator Fed Through an Electronic Expansion Valve.," *Intl. Jnl. of Enrgy. Resrch.*, vol. 21 no. 9, pp. 793-807, 1997.

[8] Rasmussen, H., Claus, T., and Larsen L., "Nonlinear Superheat and Evaporation Temperature Control of a Refrigeration Plant," *IFAC ESC 2006: Enrgy Svgs. Cont. in Plants and Bldgs.*, pp. 251-254, 2006.

[9] Singhal, A. and Salsbury, T., "Characterization and Cancellation of Static Nonlinearity in HVAC Systems," *ASHRAE Trans.*, vol. 113, pp. 391-399, 2007.

[10] Willatzen, M., Pettit, N., and Ploug-Sørensen, L., "A general dynamic simulation model for evaporators and condensers in refrigeration. Part I: moving-boundary formulation of two-phase flows with heat exchange," *Intl. Jnl. of Refrigeration*, vol. 21, pp. 398-403, 1998.

[11] He, X., Liu, S., and Asada, H., "Modeling of vapor compression cycles for multivariable feedback control of HVAC systems," *Jnl. of Dyn. Sys. Meas. and Cont.*, vol. 119, pp. 183-191, Jun 1997.

[12] Gnielinski, V., "New Equations for Heat and Mass-Transfer in Turbulent Pipe and Channel Flow," *Intl. Chem. Engr.*, vol. 16, pp. 359-368, 1976.

[13] Rasmussen, B., "Dynamic Modeling and Advanced Control of Air Conditioning and Refrigeration Systems," thesis, Univ. of Illinois, Urbana-Champaign, IL, 2005.

[14] Wattelet, J.P., "Heat transfer Flow Regimes of Refrigerants in a Horizontal Tube Evaporator", thesis, Univ. of Illinois, Urbana-Champaign, IL, 1994.

[15] Dobson, M.K., Chato, J.C., "Condensation in Smooth Horizontal Tubes", *Jnl. of Heat Transfer*, vol. 120, pp. 193-213, 1998.